Software Techniques for Sensor Redundancy Management of Flight Control Systems

E. Y. Shapiro*
Lockheed-California Company, Burbank, Calif.

The feasibility of providing flight control system redundancy by means of software is under investigation in this paper. It is shown that sufficient information can be extracted from aircraft attitude sensors to allow analytic reconstruction of the SAS (Stability Augmentation System) sensor signals in the event of multiple SAS sensor failures. The sensor signal reconstruction is performed in a deterministic setting by using a Luenberger observer. A simple and efficient design procedure is presented based on Gopinath's work. As an illustrative example, the proposed sensor signal reconstruction technique is exercised on the YF-12 airplane lateral axis rigid body simulation. It is shown that, with an accurate airframe model, perfect reconstruction is feasible. In addition, it also is shown via simulation results that with imperfect knowledge of the airframe model (based on standard wind-tunnel data) the proposed reconstruction is accurate enough to have a negligible impact on the overall aircraft performance.

I. Introduction

THE demand for high performance in modern aircraft has gradually led to acceptance of the "black box" control system as an essential adjunct to the development of the required handling qualities. This is particularly true for aircraft with relaxed static stability and aircraft employing CCV (Control Configured Vehicle) concepts. So great has become the dependence on this black box that it has achieved the status of a "safety-of-flight" item. It is then quite apparent that the reliability of the automatic control system must be comparable to that of the mechanical control linkages. Once this is accepted, then it is equally apparent that the mechanical linkages are no longer required, and fly-by-wire mechanizations are completely palatable. Thus, even further performance gains are achieved by virtue of the realizable weight savings of a fly-by-wire system vs a conventional control system. The crux of the matter is the achievement of the required functional reliability.

Traditionally, the implementation approach used to provide the desired reliability has been the use of multiple channels and/or sensors with attendant selection logic. With three or more like parameters available for comparison, a voting scheme or a midvalue select approach has been used to exclude the failed parameter from influence on normal operation. Such systems are enjoying great success in vehicles such as the L-1011, the YF-12, the F-16, and the F-111. However, there are penalties in component cost, volume, power consumption, and weight for every duplication for the sake of redundancy. This includes not only the individual components and their attendant control law implementation, but also that of the selection logic. By compounding the redundancy and selection logic, the apparent gain in reliability is soon lost because of increased failure rate associated with the higher parts count. Thus, most systems of today do not exceed quadruple implementation.

With the rapid growth of digital computer technology, it has become feasible to utilize real-time digital computation for in-flight control system implementation. It is anticipated that in the 1980's computer technology will be such that most airborne computation will be accomplished digitally. By combining the power of on-line digital computation with state reconstruction techniques (Luenberger observers in the deterministic setting), the concept of reconstructing failed sensor signals becomes quite attractive. The purpose of this paper, therefore, is to investigate the possibility of increasing the functional reliability of flight control systems by using observers to reconstruct the signals of failed sensors from the redundant information provided by associated sensors that remain operational.

II. Problem Formulation

Consider the linear time invariant system ($S1$)

$$S1\begin{cases}\dot{x}=Ax+Bu & (1)\\ y=Cx+Du & (2)\end{cases}$$

where $x\epsilon R_n$, $u\epsilon R_m$, $y\epsilon R_r$, and A, B, C, and D are real constant matrices of compatible order. In addition, consider the dynamic feedback compensator ($S2$)

$$S2\begin{cases}\dot{\hat{x}}=\hat{A}\hat{x}+\hat{B}\hat{u} & (3)\\ \hat{y}=\hat{C}\hat{x}+\hat{D}\hat{u} & (4)\end{cases}$$

where $\hat{x}\epsilon R_{n_0}$, $\hat{u}\epsilon R_r$, $\hat{y}\epsilon R_m$, and $\hat{A}$, $\hat{B}$, $\hat{C}$, and $\hat{D}$ are real constant matrices of compatible order.

System $S1$ represents the airframe dynamics and system $S2$ represents the autopilot dynamics. Therefore, the cascaded closed-loop representation of the regulator comprised of $S1$ and $S2$ is obtained by augmenting Eqs. (1-4) with

$$\hat{u}=y \tag{5}$$

$$\hat{y}=u \tag{6}$$

The resulting system (Fig. 1) is thus an unforced system described by the vector differential equation[2]

$$\dot{\xi}=\psi\xi \qquad \xi(t=0)=\xi_0 \tag{7}$$

where

$$\xi=\begin{bmatrix}x\\ \hat{x}\end{bmatrix} \tag{8}$$

Presented as Paper 76-1934 at the AIAA Guidance and Control Conference, San Diego, Calif., Aug. 16-18, 1976 (in bound volume of Conference papers); submitted Sept. 27, 1976; revision received Jan. 27, 1977.

Index categories: Handling Qualities, Stability, and Control; Reliability, Maintainability, and Logistics Support.

*Advanced Development Projects. Associate Fellow AIAA.

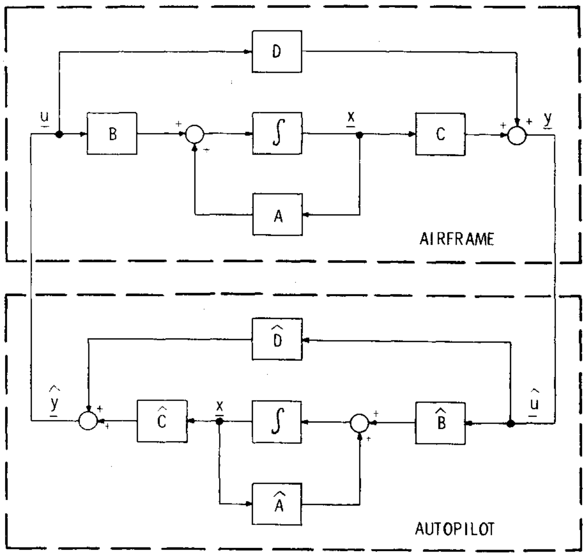

Fig. 1 Airframe/autopilot model.

and

$$\psi = \left[\begin{array}{c|c} A+B\hat{D}(I_r-D\hat{D})^{-1}C & B(I_m-\hat{D}D)^{-1}\hat{C} \\ \hline \hat{B}(I_r-D\hat{D})^{-1}C & \hat{A}+\hat{B}D(I_m-\hat{D}D)^{-1}\hat{C} \end{array} \right] \tag{9}$$

where I_k denotes the kth-order identity matrix. The presence of the inverses of $(I_r-D\hat{D})$ and $(I_m-\hat{D}D)$ does not present any problem, since it is always possible to force D to the zero matrix by including servo actuator dynamics in the airframe, thus increasing the dimension of x. (In practice, D signifies direct input/output transmission, such as lateral accelerometer response to rudder input, when rudder servo actuator dynamics are neglected.) Since, in the present study, singularity of neither $(I_r-D\hat{D})$ nor $(I_m-\hat{D}D)$ occurred, we shall adopt Eq. (9) without change.

It is assumed that system $S2$ provides acceptable response characteristics to Eq. (7), and that system $S2$ describes both the SAS and the attitude autopilot, i.e., Dutch roll damper and roll attitude.

The vector y in Eq. (2) represents the available measurements of the airframe states and usually is obtained from appropriate sensors on the aircraft. It is assumed that noise-free measurement is available, and consequently, the rest of the discussion will be carried out in a deterministic setting. Rigorous treatment of noisy sensor measurements would entail the use of Kalman filtering techniques. (In practice, typical sensor noise is sufficiently small to have negligible impact on deterministic models.) Turbulence, though random in nature, manifests itself as external perturbations. External disturbances are treated empirically in Sec. VE.

An airframe sensor failure is described by deleting the corresponding row in the C and D matrices in Eq. (2). It is therefore convenient to introduce the following notations: C_f/D_f – the C/D matrix with rows corresponding to failed sensors replaced by zero row vectors; and $\bar{C}_f/\bar{D}$ – the C/D matrix with rows corresponding to failed sensors deleted. In addition, C_c and D_c are given by

$$C_c = C - C_f \tag{10}$$

$$D_c = D - D_f \tag{11}$$

Consequently, following a sensor failure, Eq. (2) is replaced by

$$y = C_f x + D_f u \tag{12}$$

It is intended in this paper to illustrate how deterministic state reconstruction via the Luenberger observer[3] will obviate the need for triple or quadruple sensor redundancy. Thus, the required level of functional reliability can be attained without increasing weight, volume, power consumption, calibration time, etc.

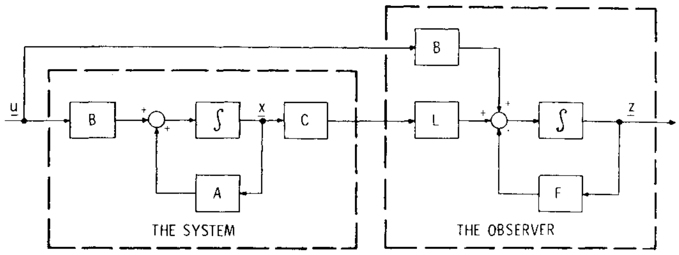

Fig. 2 The system and the observer.

III. Observer Design

In general, one might prefer to design a reduced-order observer[1,3] relative to the failed sensor problem just outlined in order to provide both simple and economical implementation. However, since no a priori information regarding future failures is available, a full-order observer[3] is employed in this discussion. To preclude the necessity for designing a bank of observers for each particular failure configuration, a single observer will be designed. This observer is driven by the airframe inputs and the outputs of sensors having the highest reliability figures. (These sensors must be backed up by hardware redundancy.)

The dynamic representation of the full-order observer (see Fig. 2) is thus

$$\dot{z} = Fz + L\bar{C}_f x + Bu \tag{13}$$

where $\bar{C}_f x$ is obtained from $\bar{y}$ of Eq. (12) by

$$\bar{C}_f x = \bar{y} - D_f u \tag{14}$$

($\bar{y}$ is the airframe output following sensor failure, $z \epsilon R_n$, $F = A - L\bar{C}_f$, and L an $n \times q$ real constant matrix.)

The evaluation of L, given the observer eigenvalues $\{\mu_i\}$ and the matrices A and $\bar{C}_f$, can be obtained easily by use of Gopinath's[1] development. Let

$$|sI - A| = s^n + a_1 s^{n-1} + \ldots a_{n-1}s + a_n \tag{15}$$

based on the desired location of the set $\{\mu_i\}$

$$|sI - A + L\bar{C}_f| = s^n + b_1 s^{n-1} \ \ldots b_{n-1}s + b_n \tag{16}$$

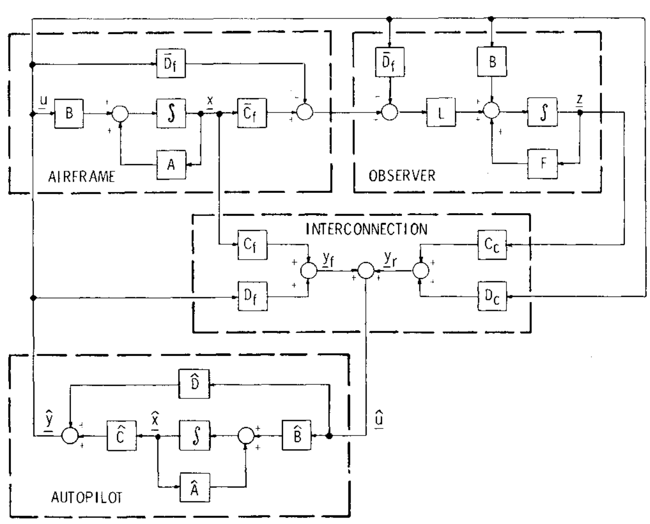

Fig. 3 The composite system.

To find an L matrix satisfying Eq. (16), define

$$a=\begin{bmatrix} a_1 \\ \bullet \\ \bullet \\ \bullet \\ a_n \end{bmatrix} \qquad b=\begin{bmatrix} b_1 \\ \bullet \\ \bullet \\ \bullet \\ b_n \end{bmatrix} \tag{17}$$

and

$$P=\begin{bmatrix} 1 & 0 & \dots & 0 & 0 \\ a_1 & 1 & \dots & 0 & 0 \\ \bullet & & & & \bullet \\ \bullet & & & & \bullet \\ \bullet & & & & \bullet \\ a_{n-2} & a_{n-3} & \dots & 1 & 0 \\ a_{n-1} & a_{n-2} & \dots & a_1 & 1 \end{bmatrix} \tag{18}$$

It then can be shown[1] that the L matrix with rank $(L)=1$ is given by

$$L=(\Gamma^{-1})^T P^{-1}(b-a)\alpha^T \tag{19}$$

where

$$\Gamma=[\bar{C}_f{}^T\alpha \mid A^T\bar{C}_f{}^T\alpha \mid \dots \mid (A^{n-1})^T\bar{C}_f{}^T\alpha] \tag{20}$$

and α is almost any vector in R_q, where q is equal to the number of rows of $\bar{C}_f$. The degree of freedom one has in selecting the vector α may be utilized to reduce the gains associated with the matrix L, while maintaining the prespecified locations of the observer poles. It is therefore possible to define a cost function $J(L)$ given by[4]

$$J(L)=\text{trace}(LQL^T) \tag{21}$$

where Q is some positive definite $q\times q$ matrix. One then may proceed to minimize $J(L)$ with respect to α subject to the constraints (19) and (20). Consequently, an observer design with "small" observer gains is obtained. However, it was found that even smaller gains are obtained if the observer gain minimization is addressed directly, namely, by selecting α subject to

$$\bar{J}(L)=\min_{\alpha}(\max_{ij}|L_{ij}|) \tag{22}$$

Minimization of Eq. (22) subject to Eqs. (19) and (20) is obtained by use of a gradient-type algorithm.

To summarize the design procedure: Eq. (20) is substituted in Eq. (19), which then is substituted in Eq. (13), allowing the determination of all of the time-invariant observer parameters (see Fig. 2).

It is important to note that the entire development thus far is based on the assumption that the aircraft behaves as a time-invariant system [Eqs. (1) and (2)], representing a fixed-flight condition. However, through the entire flight envelope the aircraft is not a time-invariant system; therefore, heuristically the observer gains have to be scheduled with air data.

It was found via digital simulation (Secs. VD and VE) that overall performance was relatively insensitive to modeling uncertainties. Thus, it is anticipated that relatively simple scheduling will provide good performance.

IV. The Composite System

For purposes of evaluating system performance in the presence of sensor failures, it is necessary to derive the composite system dynamic behavior. (By composite system is meant a system comprised of the airframe, autopilot, and observer.) Following sensor failures, the airframe dynamics are described by

$$\dot{x}=Ax+Bu \tag{23}$$

$$y=C_fx+D_fu \tag{24}$$

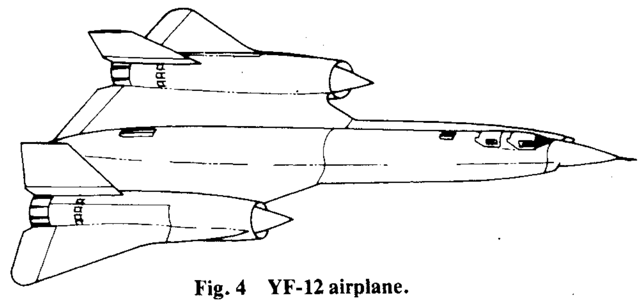

Fig. 4 YF-12 airplane.

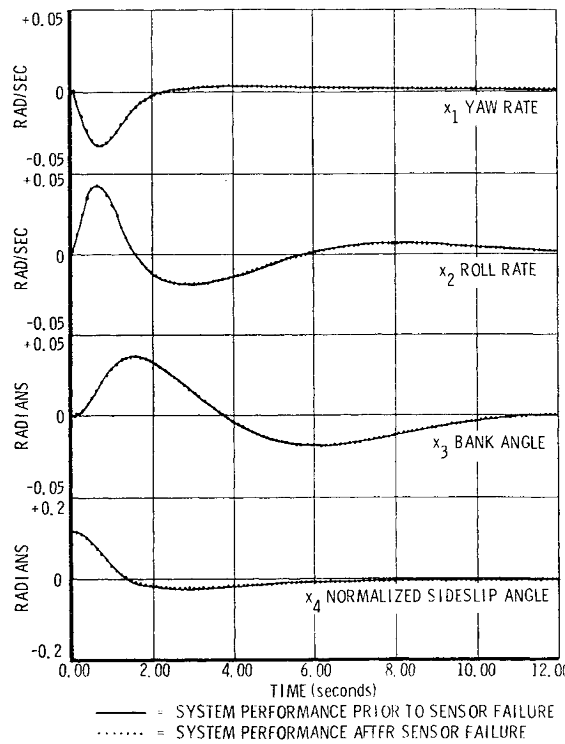

Fig. 5 System performance with perfect modeling, sensors x_1, x_2, and x_4 failed (airframe and observer initial conditions matched).

The appropriate observer is given by Eq. (13), i.e.,

$$\dot{z}=Fz+L\bar{C}_fx+Bu \tag{25}$$

and the autopilot dynamics are given by Eqs. (3) and (4):

$$\dot{\hat{x}}=\hat{A}\hat{x}+\hat{B}\hat{u} \tag{26}$$

$$\hat{y}=\hat{C}\hat{x}+\hat{D}\hat{u} \tag{27}$$

In addition, the autopilot output comprises the airframe input; thus

$$\hat{y}=u \tag{28}$$

whereas the autopilot input signal is obtained from the airframe (corresponding to sensors that did not fail) and from the observer (corresponding to failed sensors). Thus $\hat{u}$ is given by

$$\hat{u}=C_fx+D_fu+C_cz+D_cu \tag{29}$$

The block diagram of the composite system is depicted in Fig. 3.

From Eqs. (27-29) it is easy to show that

$$\begin{bmatrix} u \\ \hat{u} \end{bmatrix}=\begin{bmatrix} D & -I_r \\ I_m & -\hat{D} \end{bmatrix}^{-1}\begin{bmatrix} -C_f & C_c & 0 \\ 0 & 0 & \hat{C} \end{bmatrix}\begin{bmatrix} x \\ z \\ \hat{x} \end{bmatrix} \tag{30}$$

Table 1 Airframe parameter uncertainties

Range of variation	Parameter name
$\Delta N_r' = \pm 10\%$	Yawing moment due to yaw rate
$\Delta N_p' = \pm 100\%$	Yawing moment due to roll rate
$\Delta L_r' = \pm 100\%$	Rolling moment due to yaw rate
$\Delta L_p' = \pm 100\%$	Rolling moment due to roll rate
$\Delta N_{\delta_r} = \pm 25\%$	Yawing moment due to rudder deflection
$\Delta A_{\delta_a} = \pm 15\%$	Rolling moment due to aileron deflection
$\Delta A_{\delta_a} = \pm 15\%$	Yawing moment due to aileron deflection
$\Delta L_{\delta_r} = \pm 25\%$	Rolling moment due to rudder deflection
$\Delta Y_{\delta_r} = \pm 25\%$	Side force due to rudder deflection

Substitution of $\boldsymbol{u}$ and $\hat{\boldsymbol{u}}$ from Eq. (30) into Eqs. (23, 25, and 26) yields the vector differential equation describing the composite system, which is a regulator of the form

$$\dot{\omega} = \Pi\omega \qquad \omega(t=0) = \omega_0 \tag{31}$$

where

$$\omega = \begin{bmatrix} x \\ z \\ \hat{x} \end{bmatrix} \tag{32}$$

and

$$\Pi = \left[\begin{array}{c|c|c} A+B\hat{D}(I_r-D\hat{D})^{-1}C_f & B\hat{D}(I_r-D\hat{D})^{-1}C_c & B(I_m-\hat{D}D)^{-1}\hat{C} \\ \hline L\bar{C}_f-B\hat{D}(I_r-D\hat{D})^{-1}C_f & F+B\hat{D}(I_r-D\hat{D})^{-1}C_c & B(I_m-\hat{D}D)^{-1}\hat{C} \\ \hline \hat{B}(I_r-D\hat{D})^{-1}C_f & \hat{B}(I_r-D\hat{D})^{-1}C_c & \hat{A}+\hat{B}D(I_m-\hat{D}D)^{-1}\hat{C} \end{array}\right] \tag{33}$$

Equations (31) and (33) comprise the dynamic description of the composite system (airframe, observer, and autopilot).

V. Simulation Results

The proposed state reconstruction for the purpose of software augmentation of the airframe sensor complement was exercised on the YF-12 aircraft lateral axis rigid body simulation for a single flight condition.

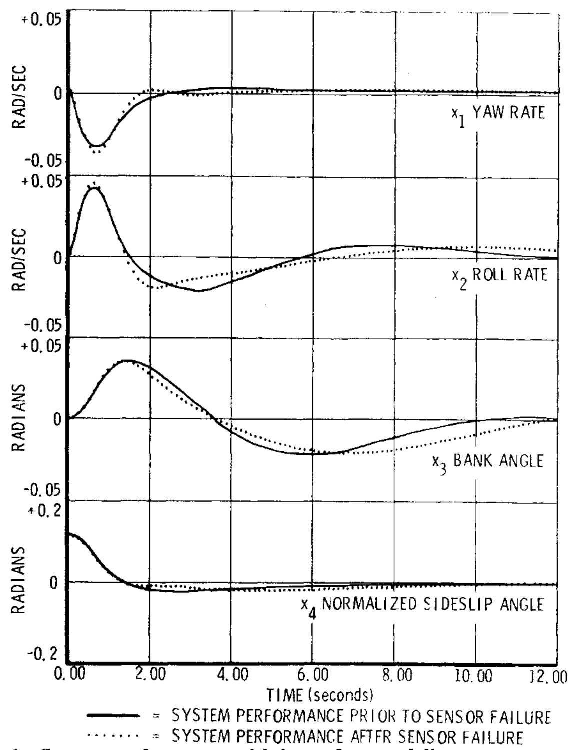

Fig. 6 System performance with imperfect modeling, sensors x_1, x_2, and x_4 failed (airframe and observer initial conditions matched).

A. Airplane Description

The two-place twin-engined YF-12 airplane (Fig. 4) is capable of extended flight at Mach numbers greater than 3.0 and at altitudes above 80,000 ft. The airplane has a delta wing planform and a long slender fuselage with prominent chines. A nacelle is mounted approximately halfway out on each wing. An all-movable vertical fin is mounted on top of each nacelle to provide directional control and stability. Pitch and roll control is provided by elevons located inboard and outboard of each nacelle. The propulsion system of the airplane consists of an axisymmetric mixed compression inlet and a J58 afterburning turbojet engine. The airplane has an air-data system which determines such parameters as Mach number, altitude, angle of attack, and angle of sideslip. An autopilot, inlet computers, and autothrottles provide automatic control for the airplane and inlets.

B. Equations of Motion

The lateral axis linearized perturbation equations, corresponding to cruise condition, are in the form of Eqs. (1) and (2), where the state $\boldsymbol{x}$ is comprised of[5] yaw rate, roll rate, bank angle, and normalized sideslip angles as denoted by x_1, x_2, x_3, and x_4, respectively. The two-component control vector $\boldsymbol{u}$ is comprised of u_1 (rudder deflection) and u_2 (aileron deflection).

For cruise flight condition, the quadruple A, B, C, D is given by

$$A = \begin{bmatrix} -0.0278 & 0.014 & 0 & -0.368 \\ 0.0331 & -0.159 & 0 & 0.637 \\ 0 & 1 & 0 & 0 \\ 3.326 & 0 & -0.037 & -0.037 \end{bmatrix} \tag{34}$$

$$B = \begin{bmatrix} -1.403 & 0.0866 \\ 1.388 & -2.969 \\ 0 & 0 \\ -0.032 & 0 \end{bmatrix} \tag{35}$$

$$C = I_4 \tag{36}$$

$$D = \begin{bmatrix} 0 & 0 \\ 0 & 0 \\ 0 & 0 \\ 0.866 & 0 \end{bmatrix} \tag{37}$$

The autopilot $\hat{A}$, $\hat{B}$, $\hat{C}$, and $\hat{D}$ of Eqs. (3) and (4) are given by

$$\hat{A} = \begin{bmatrix} 0 & 1 & 0 & 0 \\ -4.524 & -14.21 & 0 & 0 \\ 0 & 0 & -5.0 & 0 \\ 0 & 0 & 0 & -17.86 \end{bmatrix} \tag{38}$$

$$\hat{B} = \begin{bmatrix} 0 & 0 & 0 & 0 \\ 8.598 & 0 & 0 & 0 \\ 0 & 0 & 0 & 2.618 \\ 0 & 3.571 & 2.231 & 0 \end{bmatrix} \tag{39}$$

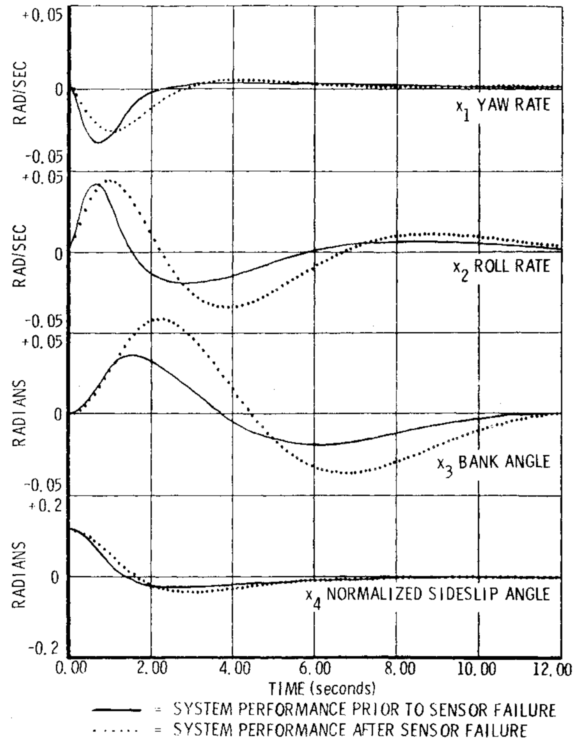

Fig. 7 System performance with perfect modeling, sensors x_1, x_2, and x_4 failed (observer initial conditions set to zero).

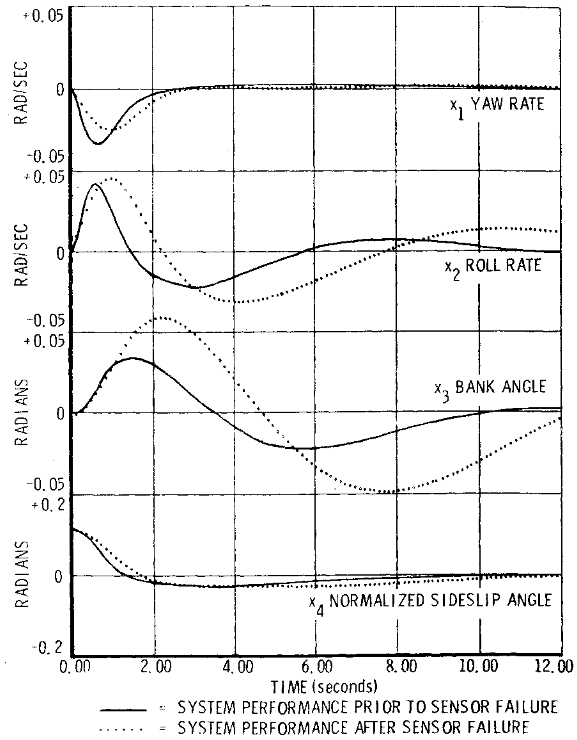

Fig. 8 System performance with imperfect modeling, sensors x_1, x_2, and x_4 failed (observer initial conditions set to zero).

$$\hat{C} = \begin{bmatrix} 0 & 3.07 & 1 & 0 \\ 0 & 0 & 0 & 1 \end{bmatrix} \tag{40}$$

$$\hat{D} = 0 \tag{41}$$

For this example, since $\hat{D}$ is equal to the null matrix, the matrix ψ of Eq. (9) is given by

$$\psi(\hat{D}=0) = \left[\begin{array}{c|c} A & B\hat{C} \\ \hline \hat{B}C & \hat{A}+\hat{B}D\hat{C} \end{array}\right] \tag{42}$$

The eigenvalues of the A matrix (34) are

λ_1	$= -0.001076$	(spiral divergence)
λ_2	$= -0.1533$	(roll subsidence)
$\lambda_{3,4}$	$= -0.03483 \pm j.1106$	(Dutch roll)

and the eigenvalues of the closed-loop regulator (42) are

$\lambda_{1,2}$	$= -0.3763 \pm j.5122$	(roll mode)
$\lambda_{3,4}$	$= -2.1119 \pm j2.8452$	(Dutch roll)
λ_5	$= -0.5187$	
λ_6	$= -0.8709$	(control poles)
λ_7	$= -11.39$	
λ_8	$= -17.26$	

C. Failure Simulation

For purposes of simulating multiple sensor failures, it is assumed that all three SAS sensors have failed, leaving only the roll attitude sensor for the bank angle Φ. (Measurement of Φ is obtained from an inertial navigation system.) Consequently, $\bar{C}_f$ is given by

$$\bar{C}_f = (0 \quad 0 \quad 1 \quad 0) \tag{43}$$

and $\bar{D}_f$ is the 1×2 null matrix.

The pair $\{A, \bar{C}_f\}$ was found to be observable, thus guaranteeing the ability to arbitrarily place the poles of the matrix $(A - L\bar{C}_f)$. The observer poles $\{\mu_i\}$ were selected to be somewhat to the left of the open-loop eigenvalues. Thus, with $\{\mu_i\} = [-1, -1.1, -1.2, -1.3]$, use of Eq. (19) with $\alpha = 1$ resulted in

$$L = \begin{bmatrix} 2.827 \\ 5.693 \\ 4.375 \\ 0.242 \end{bmatrix} \tag{44}$$

D. Parameter Variations

To evaluate the performance of the observer in the presence of parameter variations, the airframe parameter uncertainties (based on discrepancies of wind-tunnel measurements and flight test data) were calculated and are given in Table 1. These parameter uncertainties then were converted into matrix variations ΔA and ΔB, where

$$\Delta A = \begin{bmatrix} 0.003 & -0.014 & 0 & 0 \\ 0.033 & -0.159 & 0 & 0 \\ 0 & 0 & 0 & 0 \\ 0 & 0 & 0 & 0 \end{bmatrix} \tag{45}$$

$$\Delta B = \begin{bmatrix} \pm 0.351 & \pm 0.013 \\ \pm 0.347 & \pm 0.445 \\ 0 & 0 \\ \pm 0.008 & 0 \end{bmatrix} \tag{46}$$

To evaluate the quality of the state reconstruction in the presence of parameter uncertainties, the matrices $A + \Delta A$ and $B + \Delta B$ replaced the matrices A and B, respectively, in the first row only of the matrices ψ and Π of Eqs. (9) and (33), respectively. It should be emphasized that parameter variations were introduced after the observer was designed using nominal parameter values. Following the insertion of parameter uncertainties into Eq. (33), Eqs. (7) and (31) were integrated by a Runge-Kutta integration routine,[6] with nonzero initial conditions on the sideslip angle and the observer state corresponding to sideslip angle. (It is assumed that

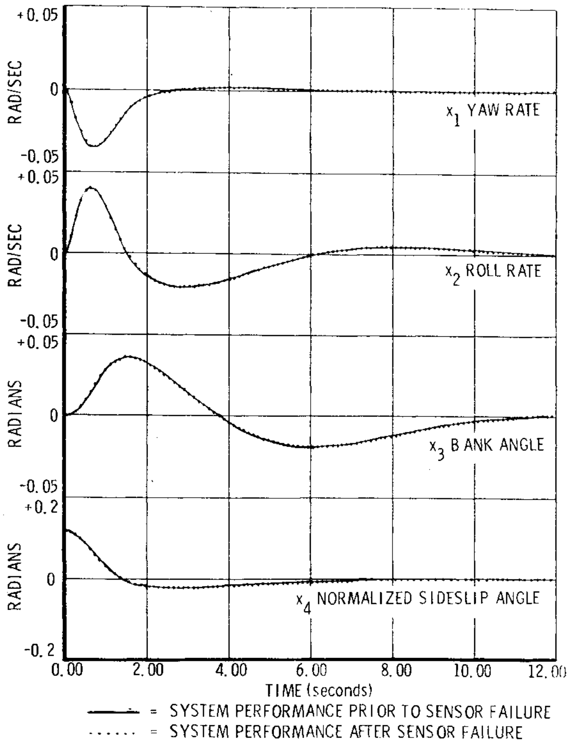

Fig. 9 System performance with perfect modeling, sensors x_1 and x_4 failed (airframe and observer initial conditions matched).

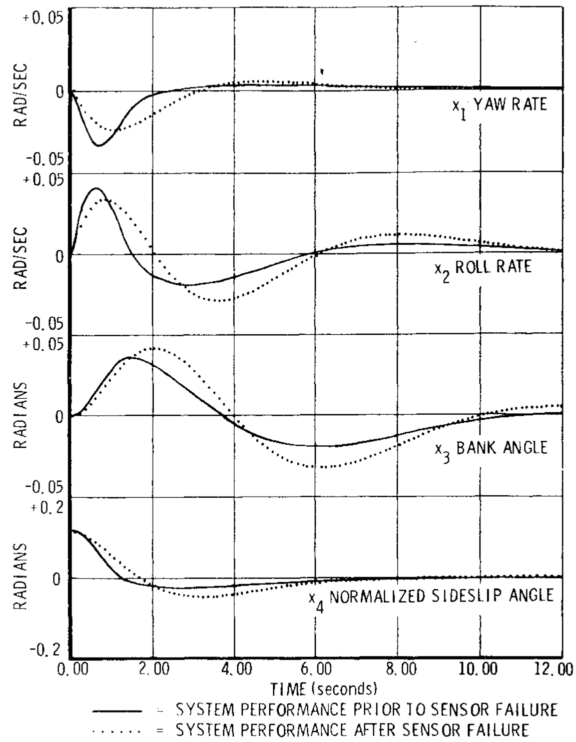

Fig. 11 System performance with perfect modeling, sensors x_1 and x_4 failed (observer initial conditions set to zero).

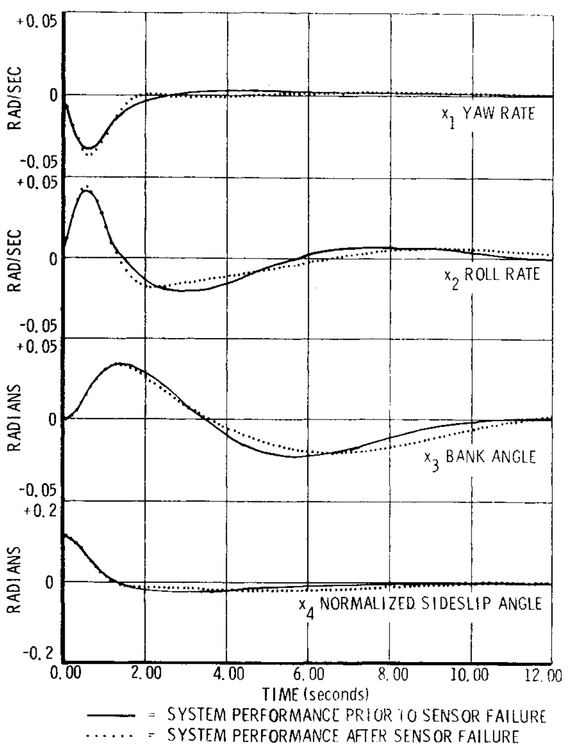

Fig. 10 System performance with imperfect modeling, sensors x_1 and x_4 failed (airframe and observer initial conditions matched).

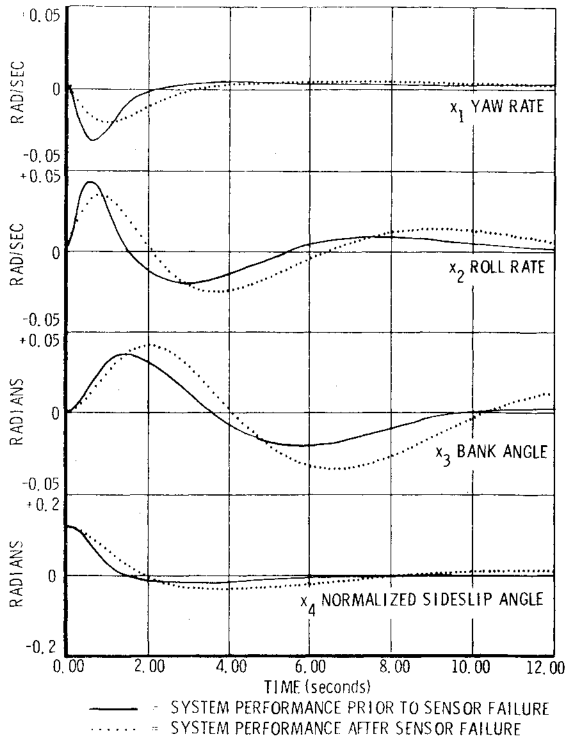

Fig. 12 System performance with imperfect modeling, sensors x_1 and x_4 failed (observer initial conditions set to zero).

all mismatch between airframe state x and observer state z has been washed out by the time the triple sensor failure occurred.) The first four components of the solutions to Eq. (7) are superimposed over the respective four components of the solution to Eq. (31) in Figs. 5 and 6 [Fig. 5 with ΔA and ΔB set to zero, and Fig. 6 with ΔA and ΔB as in Eqs. (45) and (46)]. It is seen that with perfect knowledge of the model the observer reconstruction is precise, whereas with the presence of modeling uncertainties, negligible impact on overall system performance is introduced when observer outputs are used to replace failed sensor signals.

E. Observer Initialization

External disturbances such as gusts or wind shears are equivalent to mismatch of initial conditions between the observer and the airframe. To illustrate the performance degradation for this mismatch, Eqs. (7) and (31), corresponding to the triple sensor failure [Eqs. (43) and (44)], were integrated with nonzero initial conditions on the sideslip angle (x_4) only. The corresponding superimposed time histories, with perfect and imperfect modeling, are depicted in Figs. 7 and 8, respectively. It becomes evident that because of the unmatched initial conditions (which correspond to external perturbations that are not sensed by the observer), larger transient discrepancies between the unfailed and failed system occur.

An observer driven by two sensors was designed to reduce performance degradation due to external perturbation. This observer, corresponding to double sensor failure (sensors for x_1 and x_4 are assumed to have failed), is driven by the bank angle Φ and the roll rate p. For this design the $\bar{C}_f$ matrix is given by

$$\bar{C}_f = \begin{bmatrix} 0 & 1 & 0 & 0 \\ 0 & 0 & 1 & 0 \end{bmatrix} \tag{47}$$

and $\bar{D}_f$ is the 2×2 null matrix.

The pair $\{A, \bar{C}_f\}$ is obviously observable, and the L matrix, corresponding to the observer eigenvalues $\{\mu_i\} = [-1, -1.1, -1.2, -1.3]$, was found to be

$$L = \begin{bmatrix} -1.203 & -1.852 \\ 2.840 & 4.373 \\ 0.997 & 1.536 \\ 2.847 & 4.385 \end{bmatrix} \tag{48}$$

The airframe dynamic response in the presence of a double sensor failure, to perfect and imperfect modeling [Eqs. (45) and (46)], is depicted in Figs. 9 and 10 for matched airframe and observer initial conditions, while Figs. 11 and 12 illustrate the system behavior when the airframe and observer initial conditions are unmatched, i.e., the only nonzero initial condition is on the sideslip angle. It is seen that when the observer information is increased (double sensor failure rather than triple sensor failure), the transient characteristics due to external perturbations are improved.

VI. Conclusions

Based upon analytical and simulation results, it has been shown that use of Luenberger observers is a viable method for enhancing the functional reliability of an aircraft without using conventional triple or quadruple hardware sensor redundancy. Moreover, it has also been shown, for the case of the YF-12 aircraft, that the attitude reference system contains the signal information required for reconstruction of all SAS sensor signals, and consequently this available signal information may be considered equivalent to redundant SAS sensor signals. In conclusion, it is worthy of mention that similar results were obtained relative to the L-1011 aircraft.

References

[1] Gopinath, B., "On the Control of Linear Multiple Input-Output Systems," *Bell System Technical Journal*, Vol. 50, March 1971, pp. 1063-1081.

[2] Shapiro, E. Y., "Software Techniques for Redundancy Management of Flight Control Systems," Lockheed Rept. LR-27415, Dec. 1975.

[3] Luenberger, D. L., "An Introduction to Observers," *IEEE Transactions on Automatic Control*, Vol. AC-16, Dec. 1971, pp. 596-602.

[4] Lee, G. and Jordan, D., "Pole Placement with Feedback Gain Constraints," *Proceedings of the 1975 IEEE Conference on Decision and Control*, Houston, Texas, Dec. 1975, pp. 188-190.

[5] McRuer, D. T., Bates, C. L., Ashkenas, I. L., "Dynamics of the Airframe," Navy Bureau of Aeronautics Rept. AE-61-411, 1952.

[6] Jacusiel, P., and Stern, T. E., "Variable Step Fourth Order Runge-Kutta Integration," System Research Group Tech. Rept. No. 112, Department of Electrical Engineering, Columbia University, New York, Aug. 1969.